Enhanced Linear Sampling Method for GPR Imaging

Xiang Liu, Mohammed Serhir, Abelin Kameni, Marc Lambert, Lionel Pichon

▶ **To cite this version:**

Xiang Liu, Mohammed Serhir, Abelin Kameni, Marc Lambert, Lionel Pichon. Enhanced Linear Sampling Method for GPR Imaging. International Workshop on New Computational Methods for Inverse Problems (NCMIP 2016), May 2016, Cachan, France. ⟨hal-01341986⟩

HAL Id: hal-01341986

https://centralesupelec.hal.science/hal-01341986v1

Submitted on 23 Jul 2020

HAL is a multi-disciplinary open access archive for the deposit and dissemination of scientific research documents, whether they are published or not. The documents may come from teaching and research institutions in France or abroad, or from public or private research centers.

L'archive ouverte pluridisciplinaire **HAL**, est destinée au dépôt et à la diffusion de documents scientifiques de niveau recherche, publiés ou non, émanant des établissements d'enseignement et de recherche français ou étrangers, des laboratoires publics ou privés.

HAL Authorization

Enhanced Linear Sampling Method for GPR Imaging

X. Liu, M. Serhir, A. Kameni, M. Lambert, L. Pichon

GeePs — Group of electrical engineering - Paris, UMR CNRS 8507, CentraleSupélec, Univ. Paris-Sud, Université Paris-Saclay,
Sorbonne Universités, UPMC Univ Paris 06
3 & 11 rue Joliot-Curie, 91192 Gif-Sur-Yvette Cedex, France

E-mail: xiang.liu@supelec.fr

Abstract. In this paper we consider the electromagnetic inverse scatting problem for GPR application. The reconstruction of the shape of buried dielectric objects is obtained using the well-known non iterative inverse technique entitled Linear Sampling Method (LSM). The applicability of LSM for GPR imaging is discussed, its performance with full and limited aperture is explored in a simple 2D free space configuration in a first step. The use of non-ideal sources and the possible influence of the antenna radiation pattern onto the results are considered. An enhanced approach is proposed to improve the robustness of the LSM with non-ideal sources.

1. Introduction

The Ground Penetrating Radar (GPR) technique is constantly used in geophysics and civil engineering to provide effective and accurate imaging of underground structures and for buried objects detection. It still needs development as shown by the recent (2013) start of the COST Action TU1208 entitled "Civil Engineering Application of Ground Penetrating Radar" [1, 2, 3]; Therefore, it is very interesting to improve the GPR performance for estimating the target location, size and shape. The migration techniques are the traditional GPR imaging approaches. They are able to derive relatively high-resolution images but their capability of shape reconstruction is limited. Iterative inverse scattering methods based on the solution of a nonlinear minimization problem are commonly applied because of high accuracy. However, this kind of approaches requires forward solver for an iterative minimization scheme, which is extremely complex and computational expensive for GPR application. In addition, the iterative scheme may suffer from the presence of false solution (local minima) affecting the reconstruction validity.

Other kind of inverse scattering approaches named "qualitative methods" are available. The Linear Sampling Method (LSM) is considered in this framework. LSM can reconstruct the geometrical features of both dielectric and metallic targets with few a priori information [4, 5]. Furthermore, LSM is very effective in terms of computational requirement which is very attractive in GPR surveys [6, 7]. Several successful examples are available in the literature concerning the GPR imaging via LSM by assuming the antennas as point sources, so that the antenna radiation pattern is not considered.

In this work, the feasibility and reliability of LSM for GPR application are firstly investigated in 2D situation. The synthetic multi-frequency and multi-static data is obtained using 2D Method of Moments (MoM). The non-ideal sources and the influence of the antenna radiation

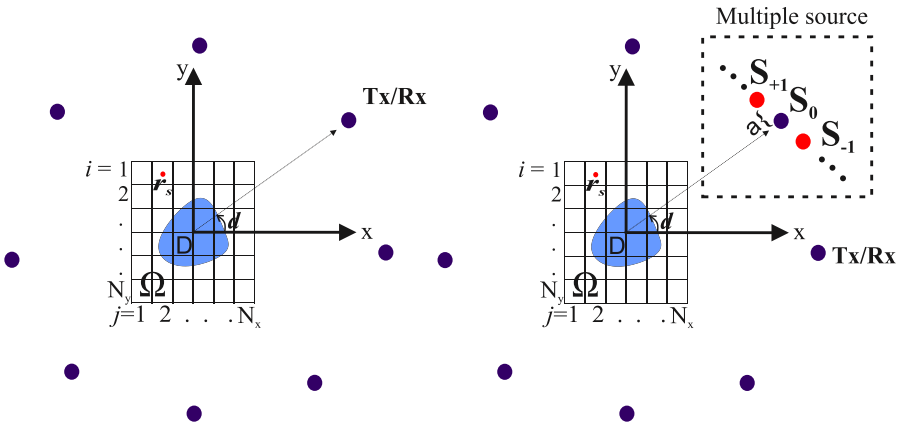

(a) Illuminated by a set of ideal sources (b) Illuminated by a set of complex sources

Figure 1. Scattering problem configuration

pattern onto the results are discussed. An enhanced algorithm is proposed to improve the LSM performance with non-ideal sources.

2. The linear sampling method

In this section, we briefly introduce the LSM for resolving the time harmonic inverse electromagnetic obstacle scattering problem.

2.1. LSM in short

Let us considerer a dielectric obstacle $D \in \mathcal{R}^2$ with $\mathcal{C}^2$-continuous boundary ∂D as shown in Fig. 1(a). For a given incident electromagnetic wave field u^i injected by a transmitter $\mathrm{T_x}$, a scattering field u^s will be caused by the presence of D. The total field is defined by $u = u^i + u^s$, which should satisfy the Helmholtz system [8].

LSM is based on solving the far field equation for the unknown $g_{\mathbf{r}_s} \in \mathcal{L}^2(\Omega)$ at each sampling position $\mathbf{r}_s$ [4, 5]:

$$\int_{\Omega} u_\infty(\hat{\mathbf{r}}, \hat{\mathbf{d}}) g_{\mathbf{r}_s}(\hat{\mathbf{d}}) \mathrm{d}s(\hat{\mathbf{d}}) = \Phi_\infty(\hat{\mathbf{r}}, \mathbf{r}_s) \tag{1}$$

where $\hat{\mathbf{r}}$ is the observation direction ($\mathrm{R_x}$ in Fig. 1(a)), $\hat{\mathbf{d}}$ denote the incident direction, u_∞ present the far field pattern of the scattered field u^s, and Φ_∞ is the far field of a point source,

$$\Phi_\infty(\hat{\mathbf{r}}, \mathbf{r}_s) = \frac{e^{i\pi/4}}{\sqrt{8\pi k}} e^{-ik\hat{\mathbf{r}}\cdot\mathbf{r}_s} \tag{2}$$

The $\mathcal{L}^2$ -norm of $g_{\mathbf{r}_s}$ becomes unbounded if the sampling point is outside the scatterer D. Therefore the indicator function of mono-frequency LSM can be defined by

$$X(\mathbf{r}_s) = \|g_{\mathbf{r}_s}\|^{-1}_{\mathcal{L}^2(\Omega)} \tag{3}$$

Then eq. (1) is approximated using the trapezoidal rule leading to

$$\boldsymbol{A} \cdot \boldsymbol{g}_{\mathbf{r}_s} = \boldsymbol{b}_{\mathbf{r}_s} \tag{4}$$

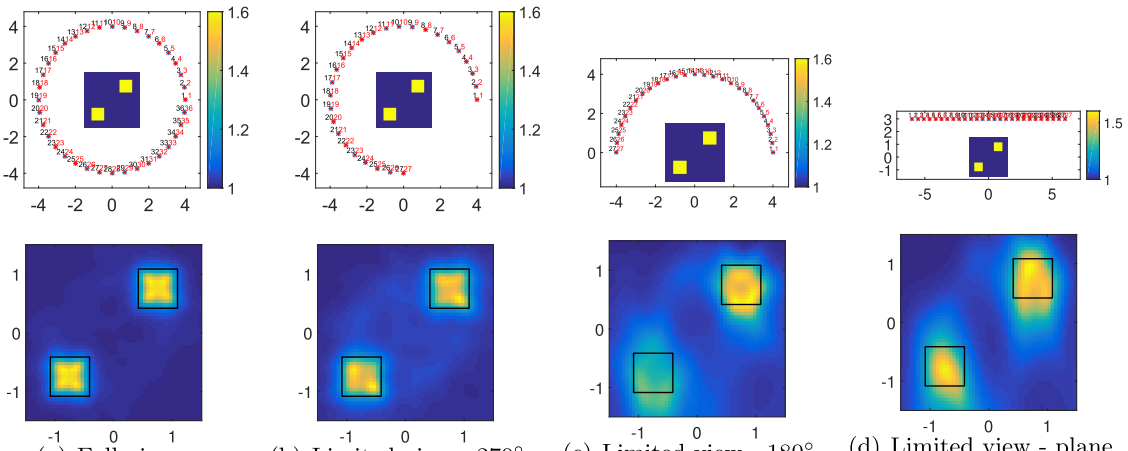

(a) Full view (b) Limited view - 270° (c) Limited view - 180° (d) Limited view - plane

Figure 2. Configuration of inverse scattering problem (top) and LSM imaging results (bottom) for various acquisition configurations: (a) full view (360°) $M = N = 36$, (b) Partial view (270°) $M = N = 27$, (c) Partial view (180°) $M = N = 27$, (d) planar configuration $M = N = 27$.

where $\boldsymbol{A}$ is the $M \times N$ multi-static matrix obtained by GPR measurement or numerical simulation, $\boldsymbol{b}_{\mathbf{r}_s}$ is given by $\frac{N}{2\pi}\phi_\infty\left(\hat{\mathbf{d}}_l, \mathbf{r}_s\right)$ using eq. (2), $1 \leq l \leq N$, M and N are respectively the number of transmitters and receivers.

Eq. (4) can be solved using Tikhonov regularization via the singular value decomposition of $\boldsymbol{A}$ [9]. Note $\boldsymbol{A} = \boldsymbol{U}\boldsymbol{S}\boldsymbol{V}^*$, and let σ denote its singular value, the $\boldsymbol{g}_{\mathbf{r}_s}$ is given by

$$\|\boldsymbol{g}_{\mathbf{r}_s}\|^2 = \sum_{p=1}^{N}\left(\frac{\sigma_p}{\alpha_{\mathbf{r}_s} + \sigma_p^2}\right)^2 |\left(\boldsymbol{U}^*\boldsymbol{b}_{\mathbf{r}_s}\right)_p|^2 \tag{5}$$

the regularization parameter $\alpha_{\mathbf{r}_s}$ being determined by Morozov principle for each sampling point [9]. By using the multi-frequency data with L operating frequencies, the multi-frequency indicator function is given by [10]

$$\boldsymbol{X}_{Mul} = \sum_{i=1}^{L} \|\boldsymbol{g}_{\mathbf{r}_s}\|_i^{-1} \tag{6}$$

2.2. Numerical results of LSM

A 2D example with two dielectric squares is firstly considered in Fig 2(a). The blue area is the grid region Ω ($3\,\mathrm{m} \times 3\,\mathrm{m}$), the transmitters/receivers are placed over a circle with radius $= 4\,\mathrm{m}$ and $M = N$. The side of the target is $0.6\,\mathrm{m}$ and its relative permittivity is 1.6, the coordinates of their centers are respectively $(0.75\,\mathrm{m}, 0.75\,\mathrm{m})$ and $(-0.75\,\mathrm{m}, -0.75\,\mathrm{m})$. The transmitters are ideal electric line sources. A White Gaussian noise of SNR $= 10\,\mathrm{dB}$ is added to the synthetic data obtained through a Method of Moments (MoM) for 21 operating frequencies from $240\,\mathrm{MHz}$ to $360\,\mathrm{MHz}$. The result is presented Fig 2(a) and shows the capability of LSM to perform a good reconstruction, while a large number of antennas is considered in the full view configuration. The LSM performance deteriorate as long as the aperture is reduced (Fig 2(b) and Fig 2(c)). A GPR surveys like configuration (plane view form) is given in Fig 2(d), the imaging result confirms the feasibility of LSM for GPR imaging problem.

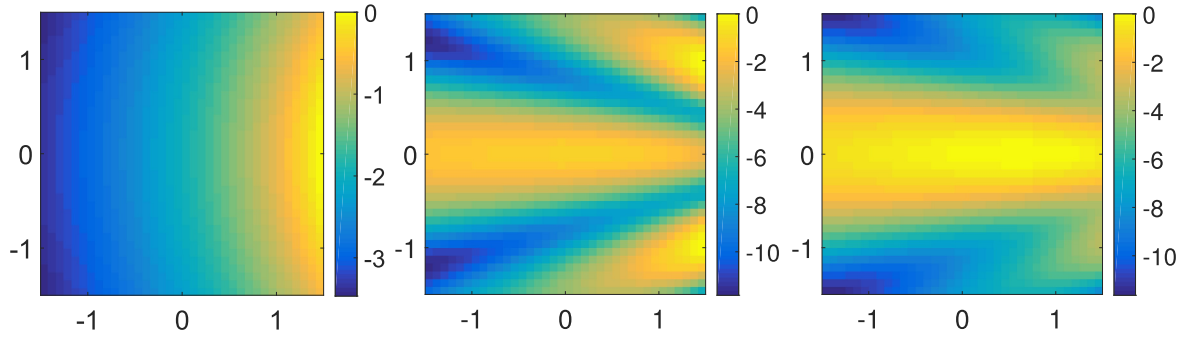

(a) $K = 1$, ideal elementary source case (b) Complex source: $K = 3$, $a = \frac{3\lambda}{2}$ (c) Complex source: $K = 5$, $a = \frac{\lambda}{2}$

Figure 3. Illumination (normalized amplitude of incident electric field E_{inc} in dB on Ω) of single source and multiple sources

3. The enforced LSM for GPR

In the classic LSM introduced in § 2, the transmitters are supposed to be ideal sources. But in most of the GPR applications, the antenna (transmitter) is a more complex source placed near the ground and is chosen such as to have a directionnal pattern which has to be taken into account in the LSM procedure.

3.1. Synthetic antenna parttern in 2D

In 2D case, A single electric line source is used to illuminate the investigated domain Ω with a classic LSM (Fig. 1(a)). The antenna pattern can be simulated using a linear combination of K ideal sources as shown in Fig. 1(b). The K ideal sources are uniformly spread on a line perpendicular to $\hat{\mathbf{d}}$ and separated by a distance a.

The normalized amplitude (in dB) of electric fields (TM mode) introduced by a single source and complex source in Ω are shown in Fig. 3 for $k = 1, 3, 5$ and for various a. The investigated domain Ω is $3\,\mathrm{m} \times 3\,\mathrm{m}$, the direction of source $\hat{\mathbf{d}} = (-1, 0)$, the distance of transmitter to the origin is $5\,\mathrm{m}$ and the signal frequency is $3\,\mathrm{MHz}$.

A comparison of the amplitude of the incident electric field (in dB) in Ω is proposed Fig. 3. It shows that the map of the incident field, as expected, strongly depend upon the choice of K and a. Comparing with the electric field emitted by a single ideal source (Fig. 3(a)), the various 2D synthetic antenna pattern can be obtained by the complex source illumination as presented Figs. 3(b) and 3(c)).

3.2. Enforced LSM

As a consequence of the antenna's pattern Ω is not uniformly illuminated while the complex source rotates. A compensation method is then proposed to improve the LSM imaging results taking into account the antenna pattern. The enforced mono-frequency LSM indicator function is defined as

$$X_E(\mathbf{r}_s) = C(\mathbf{r}_s) \cdot \|g_{\mathbf{r}_s}\|^{-1}_{\mathcal{L}^2(\Omega)} \tag{7}$$

where $C(\mathbf{r}_s)$, the compensation function, being given by

$$C(\mathbf{r}_s) = \left(\sum_{p=1}^{N} \|E_{inc}(p, \mathbf{r}_s)\| \right)^{-1} \tag{8}$$

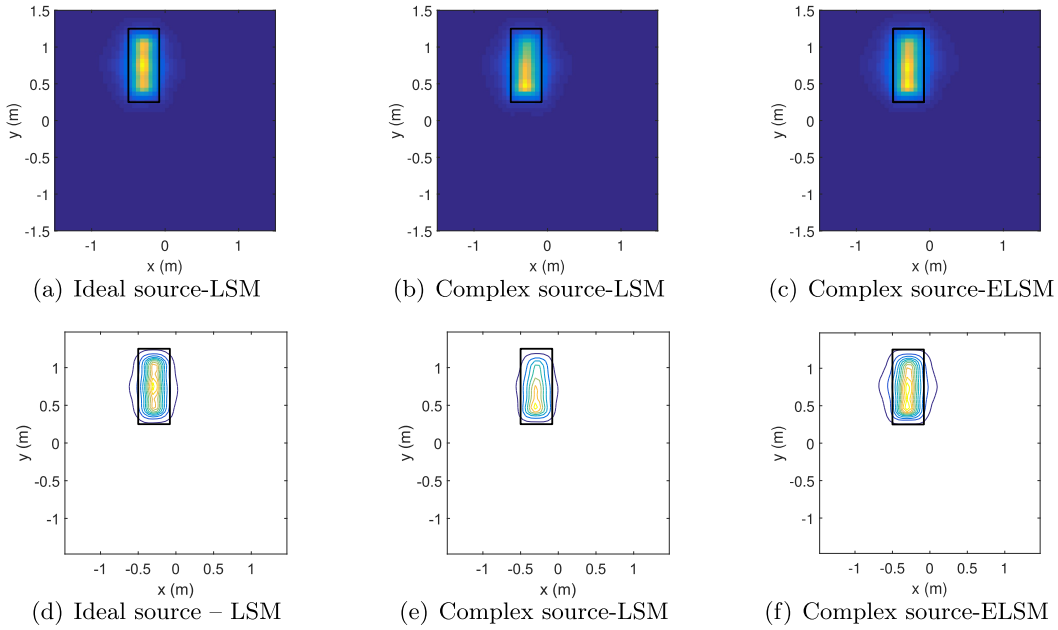

(a) Ideal source-LSM (b) Complex source-LSM (c) Complex source-ELSM

(d) Ideal source – LSM (e) Complex source-LSM (f) Complex source-ELSM

Figure 4. (a) LSM imaging result for single source illumination, (b) LSM imaging result for complex source $\left(K = 3, a = \frac{3\lambda}{2}\right)$, (c) Enforced LSM imaging result for complex source $\left(K = 3, a = \frac{3\lambda}{2}\right)$, (e) (f) (g) the respective contour plot displays of (a)(b)(c)

A result is shown in Fig. 4. The grid region Ω is 3m $\times$ 3m, the transmitters/receivers are placed over a circle with radius $= 5\,\mathrm{m}$ and $M = N = 36$. The size of the target is $0.5\,\mathrm{m} \times 1\,\mathrm{m}$, its relative permittivity is 1.6 and its center $(-0.3\,\mathrm{m}, 0.75\,\mathrm{m})$. The transmitters are either ideal electric line sources or complexe source with $K = 3$ and $a = \frac{3\lambda}{2}$. A white Gaussian noise of SNR $= 10\,\mathrm{dB}$ is added to the data obtained using a Method of Moments (MoM) at an operating frequency of $3\,\mathrm{MHz}$.

The deterioration of LSM performance with the presence of synthetic antenna pattern is observed by comparing (Fig. 4(a),4(d)) and (Fig. 4(b),4(e)). The proposed enforced LSM improves the imaging by compensating the nonuniform incident field (Fig. 4(c),4(f)).

4. Conclusion

In this framework, the feasibility of using LSM for GPR application is studied for a 2D electromagnetic problem. Preliminary results are presented in a simplified configuration. The use of non-ideal sources and the possible influence of the antenna radiation pattern onto the results is discussed. A compensation method is proposed to correct this influence. The extension of the approach to the 3D case will be dealt with and the confrontation with laboratory controlled experimentation is under investigation.

Acknowledgments

X. LIU appreciate the financial support of his PHD work by Fondation Supélec. We thank for Prof. Won-Kwang Park who provided expertise of LSM that greatly assisted this research.

References

[1] Daniels D J 2004 *Ground penetrating radar* vol 1 (Iet)

[2] Pajewski L, Benedetto A, Derobert X, Giannopoulos A, Loizos A, Manacorda G, Marciniak M, Plati C, Schettini G and Trinks I 2013 Applications of ground penetrating radar in civil engineeringcost action tu1208 *Advanced Ground Penetrating Radar (IWAGPR), 2013 7th International Workshop on* (IEEE) pp 1 – 6
[3] Benedetto A and Pajewski L 2015 *Civil Engineering Applications of Ground Penetrating Radar* (Springer)
[4] Colton D and Kirsch A 1996 *Inverse Problems* **12** 383
[5] Colton D, Haddar H and Piana M 2003 *Inverse Problems* **19** S105
[6] Catapano I, Soldovieri F and Crocco L 2011 *Prog. Electromagn. Res.* **118** 185 – 203
[7] Crocco L, Di Donato L, Catapano I and Isernia T 2013 *IEEE Trans. Antennas Propagat.* **61** 843 – 851
[8] Colton D 1992 *Inverse Acoustic and Electromagnetic Scattering Theory* (Citeseer)
[9] Colton D, Piana M and Potthast R 1997 *Inverse Problems* **13** 1477
[10] Guzina B B, Cakoni F and Bellis C 2010 *Inverse Problems* **26** 125005